STAREVOL evolution code

Amard, L. Borisov, S. Charbonnel, C. Choplin, A. Dumont, T. Faure, A. Lagarde, N. Palacios, P. Siess, L.

July 1st, 2022

Atelier code stellaire, Meudon

Generalities

- 1D lagrangian hydrodynamic code
- Dependent variables : u, lnr, lnf, lnT, L
- Solve the equation in one block from center to the photosphere
- Grey atmospheres, analytical relation T(τ) or **realistic atmospheres (PHOENIX)**.
- 2 main branches (Brussels and Geneva/Montpellier/Bordeaux/Saclay)

Main references :

- Siess et al. (2000), Siess (2006,2013)
- Palacios et al. (2003,2006), Decressin et al. (2009), Charbonnel & Lagarde (2010), Amard et al. (2016,2019), Dumont et al. (2021)

Specificities of the STAREVOL code : Equation of state

- Based on Pols et al. (1995) formalism, same family as FreeEOS.
- Minimisaation of Helmholtz free energy (lnf) with a consistent treatment of the electrons' thermodynamics and degeneracy (partial or full).
- Ionisation pressure and Coulomb screening accounted for with various analytical fits of non ideal term of Helmholtz free energy (valid up to $\Gamma \sim 300$)
- Computed at each timestep (no table interpolation)

Current developments : Implementation of a full analytical and optimised version of FreeEOS.

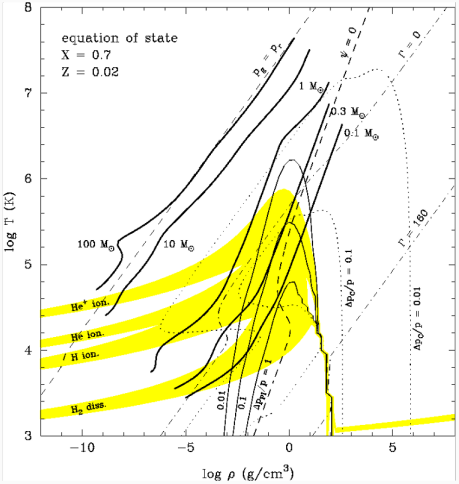

Specificities of the STAREVOL code : Opacities

Three types :

- Radiative : Mean Rosseland opacities (tabulated OPAL2.0 + Fergusson(2005) at low T°)
- Conductive : Various sources
- Molecular : For high-C giants (C/O > 1) following Marigo (2002)

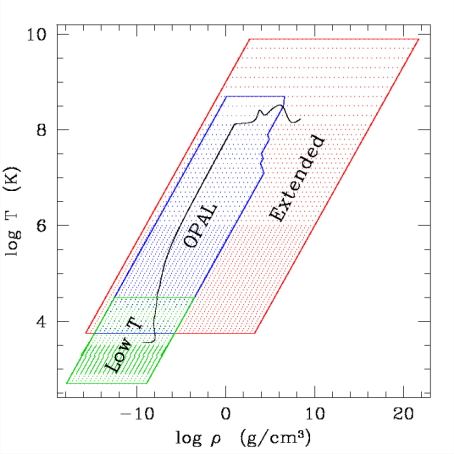

Specificities of the STAREVOL code : Nucléaires

- A 53 chemical species network (n, ^{1,2}H, ^{3,4}He, ^{6,7}Li, ^{7,9}Be, ^{8,10,11}B, ^{12,13,14}C, ^{13,14,15}N, ^{18,19,20}F, ^{20,21,22,23}Ne, ^{22,23,24,25}Na, ^{24,25,26,27}Mg, ^{26g,26m,27}Al, ^{28,29,30}Si, ^{31}P, ^{32,33,34,35,36}S, $^{3(,36,37}$Cl) and an extra 'Heavy' element which include all other species (including Fe).
- 177 nuclear reaction, including all type of interactions : nuclear (n-, p-, α captures), weak (electronic capture, β-decay) and electromagnetic (photo-disintegration).
- Brussels version : possibility to solve a 400 and a 1000 elements network to fully capture the s- and i- process

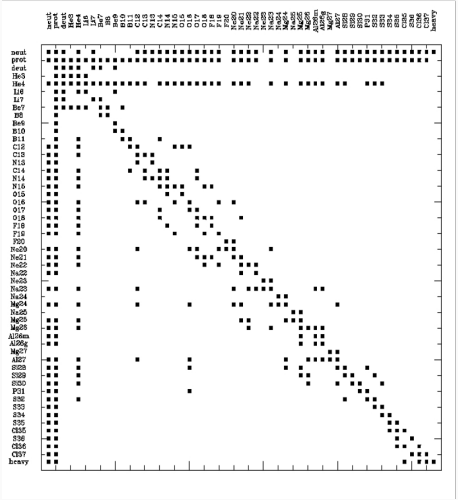

Specificities of the STAREVOL code : Transport

Transport in convective regions :

Classical Mixing-Length Theory, convective time-dependent transport (diffusion equation which include nuclear burning terms)

Transport in Radiative regions :

- Transport of matter and angular momentum according to Zahn 1992, Talon & Zahn (1997), Maeder & Zahn 1998, Maeder (2003), Mathis & Zahn 2004, Mathis et al. 2018.
- Angular momentum transport by IGW (Pantillon et al. 2008, Charbonnel et al. 2013)
- Angular momentum transport by magnetic instabilities (Spruit 2002, Fuller et al. 2019)
- Angular momentum extraction by magnetised stellar winds (Kawaler 1988, van Saders & Pinsonneault 2013, Matt et al. 2015, etc.)
- Transport of chemicals by :
  - classic overshooting
  - diffusive overshooting/penetrative convection/semi-convection (with the effect of rotation, Augustson & Mathis 2019, Baraffe et al. 2017, Korre et al. 2019, see Dumont et al. 2021)
  - thermohaline mixing (Charbonnel & Zahn 2007, Charbonnel & Lagarde 2010)
  - Atomic diffusion following Thoul et al. (1994) and collision integral computed following Paquette et al. (1986). No radiative acceleration. Voir le détail.
  - Mixing in the tachocline following Brun et al. (1999)

Specificities of the STAREVOL code : other hydrodynamical processes

Accretion of matter and energy following different scheme :

- Uniform
- Localised (ad hoc, either at surface or specific location)
- Localised and accounting for mechanical, thermal and chemical properties of the structure (Siess & Forestini 1996, 1997)

Shock wave propagation by use of an artificial viscosity

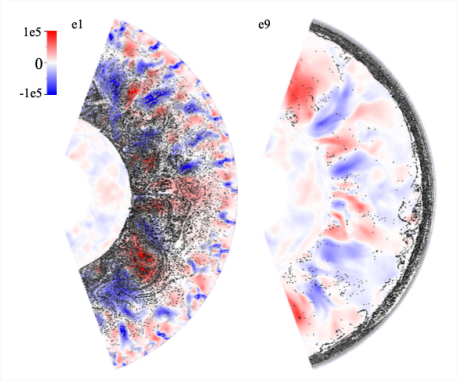

MUSIC simulations
Geroux et al. (2016)

Recent additions

- Add structural changes due to rotation (f_P,f_T factors) following Endal& Sofia (1976), Meynet & Maeder (2001)
- Improvement of chemical diffusion (Dumont et al. 2021)
- Angular momentum accretion following Ireland et al. (2020,2022) formalism
- Coupling STAREVOL & Gyre to compute consistent oscillation spectrum during model computation
- Addition of modeled atmosphere (PHOENIX) for all kind of stars
- Improvement for massive stars computation (mass-loss, remeshing)
- Switch from a SVN repository to Git repository
- Audit of the code to improve performance
- Improvement of nuclear network for AGB (up to 1200 isotopes to account for i-process) and coupling nucleosynthesis-transport for large network.
- FreeEOS equation of state now fully computed

Main recent results obtained with STAREVOL

- Low-mass stars self-consistent rotational evolution (Amard et al. 2019)
- Matching the lithium evolution in open clusters with diffusion and overshoot/penetrative convection (Dumont et al. 2021)
- Extension to low-mass stars in the Besançon Galaxy Model (Lagarde et al. 21)
- Supermassive stars evolution (Martins & Palacios 13,18,20,22)
- Extreme Helium populations in Globular clusters (Chantereau et al. 2020)
- Multiple sequence in globular clusters (Charbonnel etc)
- Role of Internal Gravity waves in PMS rotation profile (Charbonnel+13)
- Turnover timescale from PMS to RGB tip (Charbonnel+17)
- super-AGB stars - s-process & i-process (Choplin et al. 2021 e.g.)
- Binary evolution with tidal interactions and common envelope studies (BINSTAR, Siess 2013)

Low-mass stars self-consistent rotational evolution (Amard et al. 2019)

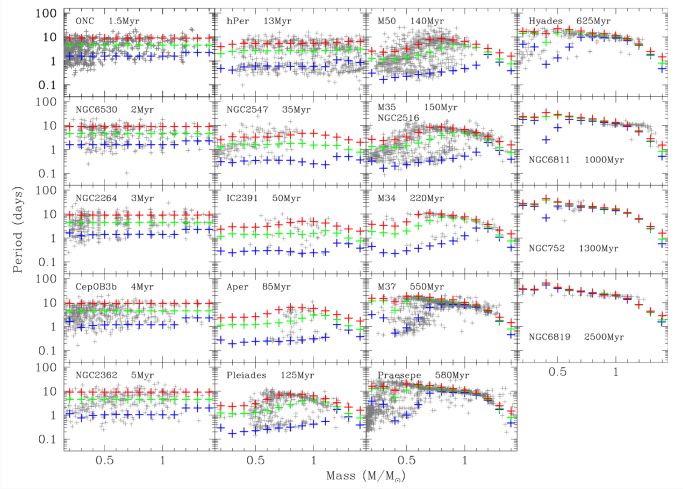

Matching the lithium evolution in open clusters with diffusion and overshoot/penetrative convection (Dumont et al. 2021)

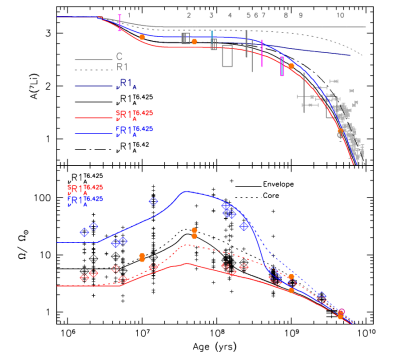

Fig. 8. Same as Fig. 1, but for the different R1 models, the selected ${}_{\nu}\mathrm{R1}_{A}^{\mathrm{T6.425}}$ model with different initial rotation velocities, and the classical model (C). The orange dots refer to the ages at which the diffusion coefficient profiles are shown in Fig. 7. The red, black, and blue open squares show the 25th, 50th and 90th percentiles of the observed rotational distributions in each cluster.

Extension to low-mass stars in the Besançon Galaxy Model (Lagarde et al. 2021)

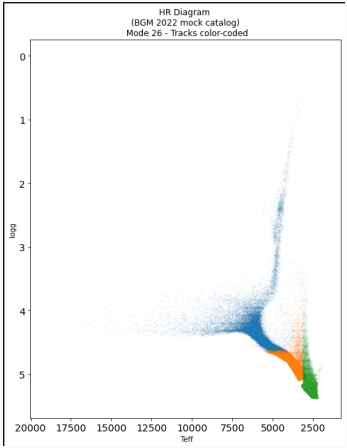

Results : High-mass stars

Massive stars evolution (Martins & Palacios 2013,2018,2021)

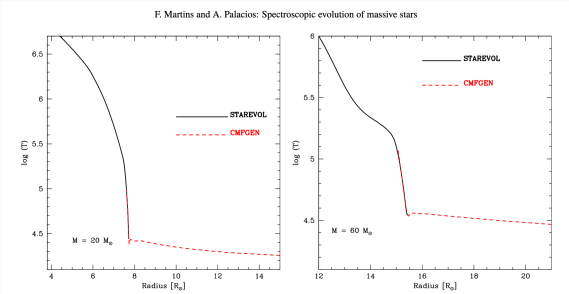

Fig. 2. Temperature as a function of radius in the evolutionary model (black solid line) and the atmosphere model (red dashed line) for representative points of the main sequence. The *left (right) panel* is for a model with $M = 20(60)\ M_{\odot}$.

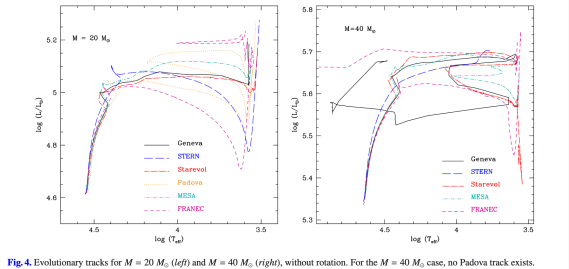

Fig. 4. Evolutionary tracks for $M = 20\ M_{\odot}$ (*left*) and $M = 40\ M_{\odot}$ (*right*), without rotation. For the $M = 40\ M_{\odot}$ case, no Padova track exists.

Supermassive stars evolution (Martins & Palacios 2022)

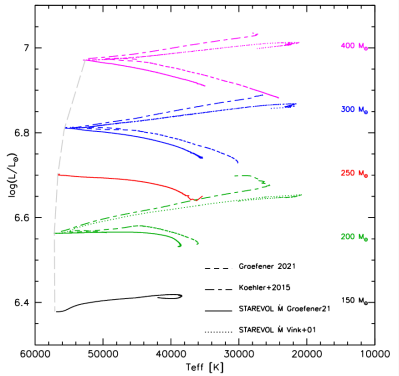

Fig. 1. Hertzsprung–Russell diagram (HRD) for our models with two different mass-loss treatments compared to those published in Köhler et al. (2015) and Gräfener (2021). See text for more details. Only the main-sequence part of the tracks up to $X_c \approx 0.01$ is shown for all models. The long dashed gray line represents the ZAMS of the *STAREVOL* models.

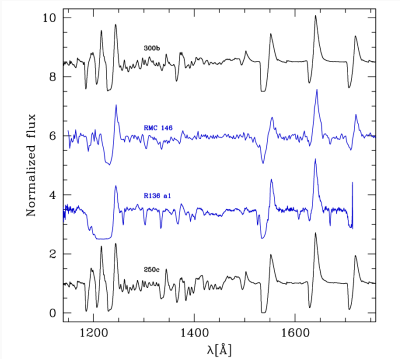

Fig. 6. UV spectrum of the WN5h stars R136 a1 and RMC 146 (blue middle spectra) with our models 250c and 300b.

Extreme Helium populations in Globular clusters (Chantereau et al. 2020)

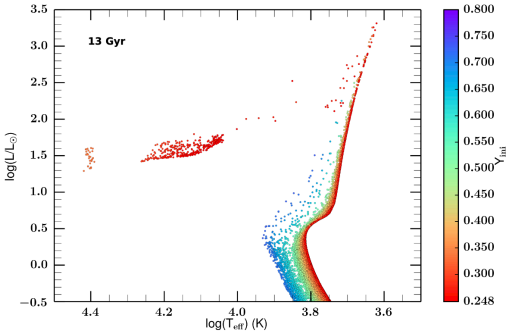

Fig. 5. Position of the synthetic GC stars in the HRD at 13 Gyr. The color code corresponds to the initial helium mass fraction of the stars that are still alive at these ages (199 887 out of the 300 000 initial sample).

Super-AGB stars - s-process & i-process (Choplin, Siess et al. 2021)

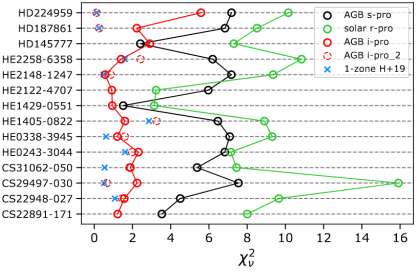

Fig. 11. Reduced χ-square values χ^2_ν of the 14 selected r/s-stars. The red, black, and green patterns show the minimum χ^2_ν values obtained with our reference *i*-process AGB model, a 2 $M_\odot$ [Fe/H] = −2.5 AGB model experiencing *s*-process and the solar scaled *r*-process from Arnould et al. (2007), respectively (see text for details). The blue crosses show the χ^2_ν values obtained with the one-zone model of Hampel et al. (2019). The dashed red circles show the results obtained with our reference *i*-process AGB model, but with the same abundance data and uncertainties as in Hampel et al. (2019, see text for details).

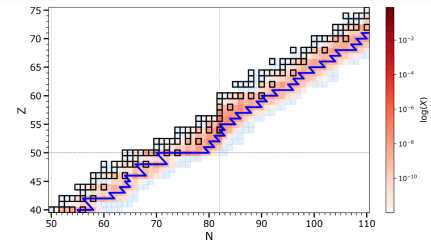

Fig. 8. Illustration of the main nuclear i-process flow (blue line) in the layer of 1 $M_\odot$, [Fe/H] = −2.5 model star with the highest neutron density of $N_n \simeq 5 \times 10^{14}$ cm^{-3}. The blue squares correspond to the nuclei included in the network, the black ones to the stable nuclei. The abundances are depicted by the red colour scale in mass fraction. The $N = 82$ isotones and $Z = 50$ isotopes are highlighted by the vertical and horizontal dotted lines, respectively.

STAREVOL models usage

Models are either found :

- On Lionel Siess' website for the oldest models, binaries and AGB models
- All the grid are available on the STAREVOL website (hosted in Geneva)
- The Amard et al. (2019) grid can also be used in Syclist, a tool to make synthetic cluster.

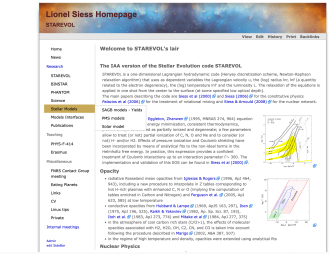

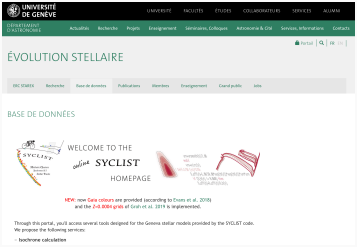

Thank you for your attention

Parameter of the Amard+19's grid

- Solar mixture : Asplund et al. (2009)
- Atmosphere models - PHOENIX (Allard et al. 2011)
- Convection : MLT, $\alpha_c = 1.973$ (Standard solar calibration 10^{-4})
- Nuclear reaction : Nacre 2
- EoS : Siess (2000) = Pols+95 improved by Dufour
- Effects of rotation on the structure (Endal & Sofia 1976)
- Mass loss rate (Reimers 1975 or Cranmer & Saar 2011 (Also estimate $\vec{B}_{eq}$))
- Internal transport : Zahn's formalism with Zahn (1992), Mathis et al. (2018)
- Angular momentum loss : Matt et al. (2015)